

Article

Mechanical Behavior of Hydrated-Lime–Liquid-Stabilizer-Treated Granular Lateritic Soils

Kangwei Tang ^{1,2}, Feng Zeng ¹, Liang Shi ^{3,*}, Long Zhu ², Zining Chen ¹  and Feng Zhang ^{2,*} ¹ China Road and Bridge Corporation, Beijing 100013, China² School of Transportation Science and Engineering, Harbin Institute of Technology, Harbin 150090, China³ Heilongjiang Provincial Highway Survey and Design Institute, Harbin 150080, China

* Correspondence: liang345@126.com (L.S.); zhangf@hit.edu.cn (F.Z.)

Abstract: Granular lateritic soil is commonly used for road construction in humid tropical and sub-tropical regions. However, the high plastic clay content and poor particle distribution of some laterite materials make them unsuitable for bases and subbases. Lime treatment is a widely used method for improving problematic lateritic soil, and liquid ionic stabilizers are considered an environmentally friendly solution for reinforcing such soils. However, using only lime or only stabilizers may not be optimal. This study investigated the effect of treating granular lateritic soil with hydrated lime and a new liquid stabilizer, Zhonglu-2A (ZL-2A). A series of indoor tests, including compaction, California bearing ratio, and unconfined compressive strength tests, were conducted to evaluate the effects of hydrated lime content and stabilizer content on the mechanical properties, mineralogical composition, and microstructure of the soil. The results show that an increase in hydrated lime dosage increases the optimal moisture content and decreases the maximum dry density. The CBR of lime-stabilizer-treated laterite was at least 2–3 times higher than that of the only-lime-treated soil. The highest CBR was observed in samples treated with 0.2% ZL-2A stabilizer. The sample with 6% lime and 0.2% ZL-2A stabilizer exhibited the highest unconfined compressive strength, and a nearly linear increase was observed between the unconfined compressive strength and CBR. Further investigation of the stabilization mechanism using X-ray diffraction mineralogy analysis and scanning electron microscopy revealed that the inorganic substances of the ZL-2A stabilizer and the hydrated lime provided the basic conditions for the reaction and generated cementitious hydrates on the clay particles. The mixture of granular lateritic soil and hydrated lime was wrapped by the ZL-2A stabilizer, forming a complex spatial structure and improving the strength of the soil. To improve the bearing capacity of subgrades in actual subgrade engineering, a combination of a liquid ionic stabilizer and lime should be used to treat laterite.



Citation: Tang, K.; Zeng, F.; Shi, L.; Zhu, L.; Chen, Z.; Zhang, F. Mechanical Behavior of Hydrated-Lime–Liquid-Stabilizer-Treated Granular Lateritic Soils. *Sustainability* **2023**, *15*, 5601. <https://doi.org/10.3390/su15065601>

Academic Editor: Ramadhansyah Putra Jaya

Received: 17 February 2023

Revised: 17 March 2023

Accepted: 18 March 2023

Published: 22 March 2023

Keywords: granular lateritic soil; hydrated lime; liquid stabilizer; unconfined compressive strength; California bearing ratio



Copyright: © 2023 by the authors. Licensee MDPI, Basel, Switzerland. This article is an open access article distributed under the terms and conditions of the Creative Commons Attribution (CC BY) license (<https://creativecommons.org/licenses/by/4.0/>).

1. Introduction

Lateritic material is a type of weathered soil that forms through the concentration of hydrated oxides of iron and aluminum, primarily in humid tropical and subtropical regions [1,2]. Due to its low cost and the limited availability of high-quality aggregates, this soil has gained attention as a potential local material for road construction purposes. Several studies have investigated the mechanical performance of granular lateritic soils and lateritic gravel, focusing on properties such as California bearing ratio (CBR), resilient modulus, compressive strength, and tensile strength [3–8]. Although laterite is commonly used in road construction projects [9–11], some types of laterites may not meet the requirements for bases and subbases due to high levels of plastic clay content and poor particle distribution. Therefore, it is necessary to improve the mechanical and physical properties of lateritic

soil, particularly its compressive strength and CBR, in order to meet the demands of road construction.

Lime treatment is a commonly used technique to improve the properties of problematic lateritic soil [12–16]. The physical and mechanical characteristics of hydrated-lime-treated soils are influenced by factors such as the quantity of hydrated lime used, the curing time, the environmental conditions, and the testing method. Osinubi [17] investigated the effects of quicklime content (ranging from 0% to 8%) on the compaction characteristics, compressive strength, and permeability of fine lateritic lime soil. The results showed that the optimum moisture content (OMC) and unconfined compressive strength (UCS) increased with increasing lime content, while the maximum dry density decreased. Millogo et al. [18] found that quicklime additions resulted in a reduction in the clayey fraction, plasticity index, methylene blue value, and maximum dry density, as well as resulting in an increase in the optimum moisture content. They recommended the use of 3% hydrated lime-modified lateritic gravels for the base course. Eisazadeh et al. [19] used solid-state nuclear magnetic resonance (SSNMR) and Fourier transform infrared (FTIR) spectroscopy to investigate the time-dependent changes in the structures of lime-stabilized lateritic clays. Tan et al. [20] reported that lime could improve the California bearing ratio (CBR) of lateritic clay when the lateritic agglomerate size was between 0.5 mm and 2 cm, while the effect was not significant when the size was between 1 cm and 6 cm. Ojuri et al. [21] used lime and cement with a ratio of 1:2 to treat lateritic soil (SC by USCS classification) and identified an LMT70-30 sample (consisting of 70% lateritic soil and 30% mine tailing) stabilized with 8% binder as the most suitable base course material.

Several types of stabilizers have been employed to improve problematic soils [22], with liquid ionic stabilizers being a promising environmentally friendly option [23–25]. These stabilizers typically induce cation exchange, which can decrease the thickness of water films and promote clay mineral flocculation, thereby altering soil particle structure [16,26]. For example, Sarkar et al. [27] treated Crowley soil with a hydrogen ion exchange chemical and observed a 35% average reduction in swell–shrink potential compared to untreated soil. Yunus et al. [28] reported that an SS299 soil stabilizer significantly increased the unconfined compressive strength and shear strength of laterite soil. Gullu et al. [29] studied a non-traditional stabilizer (synthetic fluid) used in conjunction with a geofiber to improve the UCS characteristics of low-plasticity fine-grained soil. Zhao et al. [30] found that a potassium-based stabilizer is effective in controlling the swelling potential of expansive clay. The mechanism of stabilization by ionic agents likely involves cation exchange and increases in cation concentrations in the soil pore water. Gautam et al. [31] used a liquid ionic soil stabilizer (LISS) to treat Carrollton expansive clay and observed a 53% reduction in swell when the soil was compacted at the optimal moisture content. Wu et al. [32] investigated pore and compression behaviors using an ionic soil stabilizer to treat Wuhan clay and found that it led to changes in pore direction, reductions in pore number and size, decrease in porosity, and the formation of larger aggregates.

Numerous studies have investigated the use of lime and curing agents to stabilize laterite. However, the efficacy of using either lime or a curing agent alone may be limited. Furthermore, the availability of lime in certain regions may be a challenge. Nevertheless, combining the use of lime and a curing agent can result in improved stabilization, potentially allowing for a significant reduction in lime usage. Consequently, the use of a lime-curing agent as a stabilization technology for laterite may be both cost-effective and environmentally sustainable. However, the literature currently offers limited research on the application of lime-curing agents for stabilizing laterite.

The purpose of this study was to examine the impact of hydrated lime and a new liquid curing stabilizer, ZL-2A, on granular lateritic soil by performing compaction tests, CBR tests, UCS tests, X-ray diffraction (XRD) mineralogical analysis, and SEM tests. The results of the CBR and UCS tests for the treated granular lateritic soil are compared and analyzed. Furthermore, the mineralogical and microstructural characteristics are discussed.

2. Materials and Methods

2.1. Materials

The granular lateritic soils depicted in Figure 1 were collected from the PK6 Highway in Senegal, Western Africa. These disturbed soil samples have been commonly utilized in the construction of subgrade, base, and subbase layers for highways in Senegal. The soil's basic physical parameters were evaluated in accordance with the Test Methods of Soils for Highway Engineering (JTG 3430-2020) [33]. The soil has a density of 2.8 g/cm^3 , a natural water content of 4%, an optimum moisture content of 9.2%, and a maximum dry density of 2.13 g/cm^3 , with a pH of 5.4. The liquid limit, plastic limit, and plasticity index of the granular lateritic soil were found to be 38.9%, 17.6%, and 21.3%, respectively.



Figure 1. Granular lateritic soil.

Figure 2 displays the grain size distribution of the granular lateritic soil used in this study as well as other lateritic soils utilized in other studies. The results indicate that over 70% of the laterite gravels fell in the range of 2.36 to 16 mm, with the majority of them being in the 4.75 to 9.5 mm range (32.7%). The non-uniformity coefficient and curvature coefficient for the lateritic soil used in this study were 9.2 and 2.3, respectively, classifying this soil as well-graded gravel.

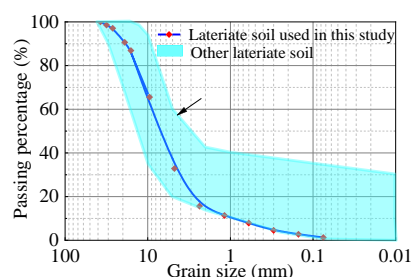


Figure 2. Grain size distribution of the granular lateritic soil sample.

Table 1 presents the major chemical components of the granular lateritic soils used in this study. The chemical components of the soil were determined using the Total Analysis Methods of Forest Soil (GB 7873-87) [34]. This method involves decomposing the minerals in the soil and creating a solution, after which the content of each mineral element is determined individually. The soil is composed mainly of SiO_2 , Al_2O_3 , and Fe_2O_3 , accounting for 24.650%, 19.500%, and 38.156% by weight, respectively. The silica–sesquioxide ($\text{SiO}_2/\text{R}_2\text{O}_3$) ratio of 0.42 classifies this soil as a true laterite. True laterites are categorized by S/R ratios below 1.33, while lateritic soils are between 1.33 and 2.00, and non-lateritic tropically weathered soils are above 2.00, based on the chemical classification system.

A comprehensive review of the relevant literature suggests that no African countries have established any regulation on the free swelling rate of laterite for their road construction projects [9], indicating that the phenomenon of free swelling in laterite is not considered a major concern in these regions. In contrast, the Brazilian specifications for laterite road construction limit the free swelling rate of natural laterite to no more than 10%. To investigate the free swelling behavior of natural laterite in African regions, ten samples were carefully selected and tested according to the Brazilian specifications. As shown in

Figure 3, the free swelling rate of natural laterite in Senegal is no more than 2.0%, which is significantly lower than the limit of 10% specified in the Brazilian regulations. This finding demonstrates that the expansion behavior of natural laterite in African regions is relatively low. Given that the addition of stabilizers to laterite enhances its stability, this study will no longer focus on the issue of laterite swelling due to water absorption.

Table 1. Chemical composition of the granular lateritic soil.

Constituent	Percentage (wt.%)	Constituent	Percentage (wt.%)
SiO ₂	24.650	Na ₂ O	0.152
Al ₂ O ₃	19.500	K ₂ O	0.094
Fe ₂ O ₃	38.156	P ₂ O ₅	0.988
CaO	0.582	TiO ₂	2.317
MgO	0.105	S	0.039
MnO	0.027	Other impurities	13.390

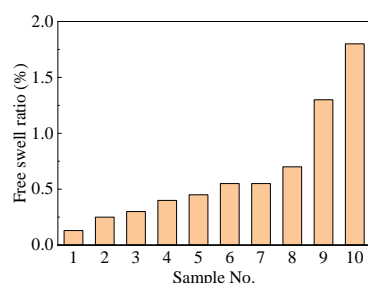


Figure 3. Free swell ratio of the lateritic soil.

The binders employed in this study were hydrated lime and a ZL-2A liquid ionic stabilizer, which were procured from Liaoning Yidan Calcium Industry Co., Ltd., Shenyang, China, and Jilin Zhonglu New Material Co., Ltd., Changchun, China, respectively. The hydrated lime had a calcium hydroxide content of 98%. The ZL-2A liquid ionic stabilizer was a dark red-brown liquid with an alkaline odor that could be fully dissolved in water. Table 2 presents a summary of the pH, density, solid content, and NaOH content of the stabilizer. The pH of the stabilizer was measured using a pH meter, while the density was determined by measuring the weight of 100 mL of the stabilizer. The solid content was measured through the oven-dry method, and the NaOH content was determined using NaOH titration.

Table 2. Properties of the ZL-2A liquid ionic stabilizer.

Properties	Value
pH	11.5
Density (g/cm ³)	1.26
Solid content (%)	33
NaOH content (%)	7.0–9.5%

2.2. Specimen Preparation

The maximum dry density and optimum water content corresponding to varying lime content were determined through a compaction test before the preparation of the specimen. The compaction test was conducted following the Test Methods of Soils for Highway Engineering (JTG 3430-2020) [33]. The granular laterite soil was first oven-dried at 60 °C for 24 h and passed through a 40 mm sieve. Distilled water was then added to the dried soil sample and mixed thoroughly. The moist mixture was transferred into a plastic bag and sealed for at least 24 h to ensure moisture homogeneity in the soil. For the hydrated lime-stabilized laterite samples, the prepared moist soil was thoroughly mixed with the designated hydrated lime. The lime content was set at 3%, 6%, and 9% (by weight)

of the dry soil, based on the research results of Osinubi [17]. The final water content for each sample was adjusted to reach the designed value. Table 3 presents the water content of the hydrated-lime-treated granular laterite soil for the modified Proctor test. As shown in Table 3, the design for the compaction test involves 4 groups with different hydrated lime content. For each group, 5 samples with different water content were prepared.

Table 3. Water content of the hydrated lime-treated soil for the modified Proctor test.

Group Number	Hydrated Lime Content		Water Content					
	/ %		/ %					
1	0	8.0	8.5	9.5	10.3	11.0	13.0	
2	3	8.0	8.5	9.5	10.3	11.0	13.0	
3	6	8.0	9.0	10.0	11.0	12.0	14.0	
4	9	8.5	9.5	10.2	11.0	12.5	14.0	

The preparation of soil specimens for testing followed the Test Methods of Soils for Highway Engineering (JTG 3430-2020) [33] standard. The hydrated lime-stabilized soil samples were prepared with a diameter of 150 mm and a height of 120 mm. A thin layer of Vaseline was applied to the inner cylinder mold to reduce friction, and the lime-treated soil was added to the mold and compacted 98 times in three layers. For the lime- and stabilizer-treated soil specimens, distilled water was first added to the raw dried granular lateritic soil sample and mixed, and then the remaining distilled water was mixed with the ZL-2A liquid ionic stabilizer according to the manufacturer's suggested proportions. The stabilizer-treated soil sample was then compacted. Table 4 provides information on the test conditions used for the hydrated lime and ZL-2A-stabilizer-treated granular lateritic soils. The hydrated lime content was set at 3%, 6%, and 9%, while the ZL-2A stabilizer content was 0‰, 0.1‰, 0.2‰, 0.3‰, and 0.5‰.

Table 4. Test conditions for the hydrated lime- and agent-treated granular lateritic soils.

No.	Symbol	Lime Content (wt.%)	ZL-2A Stabilizer Content (wt.‰)	Dry Density (g/cm ³)	Water Content (wt.%)
S0	L0C0	0	0	2.134	9.1
S1	L3C0	3	0	2.120	9.5
S2	L3C0.1	3	0.1	2.120	9.5
S3	L3C0.2	3	0.2	2.120	9.5
S4	L3C0.3	3	0.3	2.120	9.5
S5	L3C0.5	3	0.5	2.094	10.1
S6	L6C0	6	0	2.094	10.1
S7	L6C0.1	6	0.1	2.094	10.1
S8	L6C0.2	6	0.2	2.094	10.1
S9	L6C0.3	6	0.3	2.094	10.1
S10	L6C0.5	6	0.5	2.094	10.1
S11	L9C0	9	0	2.066	10.9
S12	L9C0.1	9	0.1	2.066	10.9
S13	L9C0.2	9	0.2	2.066	10.9
S14	L9C0.3	9	0.3	2.066	10.9
S15	L9C0.5	9	0.5	2.066	10.9

The treated soils were compacted, then coated with a plastic membrane, and placed in a curing chamber at a temperature of 20 ± 2 °C and a humidity of 95%. The curing duration was determined to be 7 days according to the Test Methods of Materials Stabilized with Inorganic Binders for Highway Engineering (JTG E51-2009) [35].

2.3. Test Methods

A series of CBR tests were carried out on the samples soaked for 4 days according to the Test Methods of Soils for Highway Engineering (JTG 3430-2020) [33]. The top surface

of the prepared sample was subjected to a 2.0 kg surcharge ring and loaded with a force of 45 N at a speed of 1.25 mm/min using a penetration bar. The depth of penetration was recorded by a dynamometer dial indicator with integer readings.

The UCS test was carried out according to the test methods of materials stabilized with inorganic binders for highway engineering (JTG E51-2009) [35]. After the curing duration, the specimen was immersed in water for 24 h. When the surface moisture of the specimen was air-dried, a pavement material strength tester was used with a strain rate of 1 mm/min. The stress would keep rising until the specimen was broken, when the test was terminated, and the maximum stress and strain were recorded. The maximum strain was the failure strain, and the unconfined compressive strength could be determined as Formula (1):

$$R_c = P/A, \quad (1)$$

where R_c is the unconfined compressive strength, MPa, P is the maximum stress, N, and A is the sectional area of the specimen, mm^2 .

An XRD analysis was performed on the raw soil, hydrated lime, and treated soil samples. An XRD (Empyrean) was employed in this study. To prepare the sample powder for analysis, all of the samples were first passed through a 2 mm sieve, then fully ground using a mortar, passed through a 325-mesh sieve ($45 \mu\text{m}$), evenly spread on a glass plate, and placed on the scanning table. The scanning parameters were as follows: drive shaft 1theta–2theta linkage, a scanning range of 10–70, a continuous scanning mode, a scanning speed of $2.0000^\circ/\text{min}$, and a sample tilt of 0.0500° . The adjustment time was 1.50 s.

SEM was used to elucidate the high-resolution microstructure of the soil. An SEM (MERLIN Compact) with a secondary electron image resolution of 0.8 nm was employed in this study. Prior to SEM testing, the soil sample was ground into a powder with a mortar, and then a small amount was taken with tweezers or toothpicks and placed on the conductive adhesive to ensure that the adhesive was firm and dust-free. The conductive adhesive was carefully attached to the metal sheet in advance with a maximum diameter of 30 mm. The sheet metal was placed together with the sample in the box with double-sided adhesive tape on standby to prevent shaking. Gold spraying was required for sample preparation for approximately 15 min after vacuuming. The sample was then placed on the platform for observation.

2.4. Flowchart

Figure 4 illustrates the methodology employed in this study. As depicted in the figure, natural laterite specimens were prepared by mixing lime and curing agent either separately or simultaneously. The resulting test pieces were subjected to curing and soaking procedures, followed by testing for California bearing ratio (CBR) and unconfined compressive strength (UCS), respectively. Subsequently, X-ray diffraction (XRD) and scanning electron microscopy (SEM) analyses were performed on the samples.

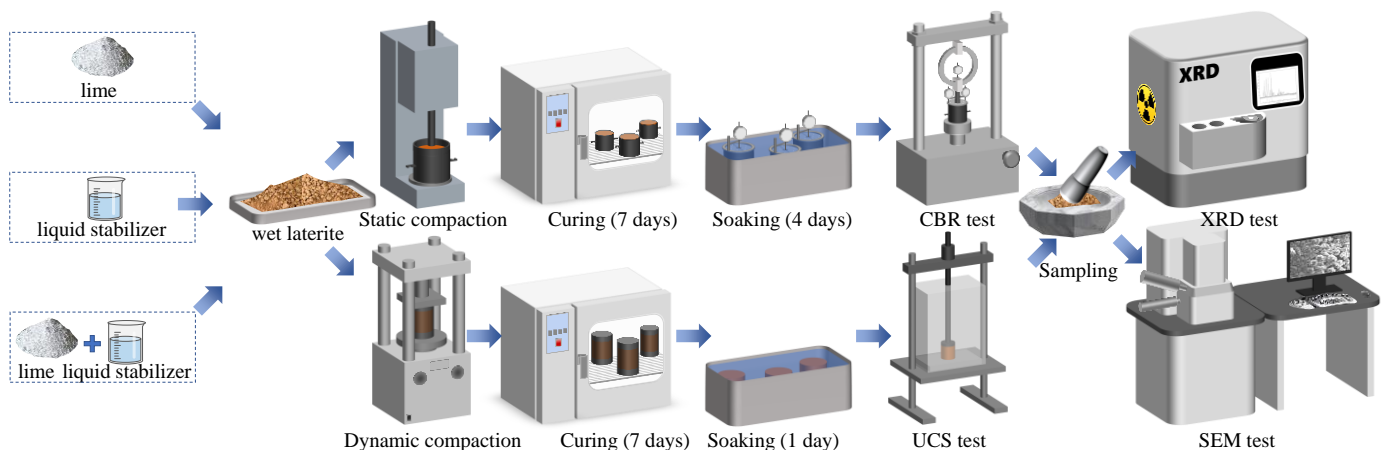


Figure 4. Flowchart.

3. Results

3.1. Maximum Dry Density and Optimal Moisture

Figure 5 displays the correlation between the water content and the dry density of the granular lateritic soil with varying lime contents. Figure 6 illustrates the impact of lime content on the maximum dry density and the optimal moisture content of the granular lateritic soil. The raw granular lateritic soil had an optimal moisture content of 9.2% and a maximum dry density of 2.13 g/cm³. Upon increasing the hydrated lime dosage to 3%, 6%, and 9%, the optimal moisture content increased to 9.5%, 10.1%, and 10.9%, respectively. In contrast, the maximum dry density slightly decreased to 2.12, 2.10, and 2.07 g/cm³, respectively. This trend is consistent with the findings of Osinubi [17] and Millogo et al. [18]. This is mainly due to the fact that the density of hydrated lime is lower than that of plain soil, and the consolidation of hydrated lime addition is not evident at the beginning, resulting in a smaller maximum dry density of the solidified soil than that of the plain soil.

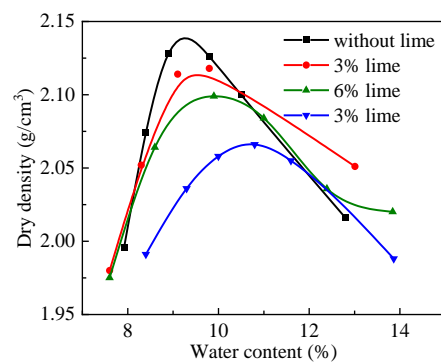


Figure 5. Compaction curves of laterite with varying lime content.

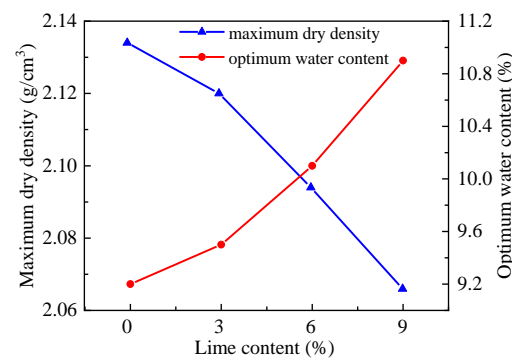


Figure 6. Variations in the optimum moisture content and maximum dry density of laterite with the change in lime content.

3.2. CBR

Figure 7 illustrates the CBR results obtained for both the raw and treated granular lateritic soils. The raw soil had a CBR of 79%, which is slightly below the minimum requirement of 80% for low-volume roads in Africa [9] and does not satisfy the specifications for the base and subbase of high-grade or heavy traffic highways (JTG/T F20-2015). However, after the addition of the binder, the CBR of all treated soils increased above 80% and even exceeded 160%, which is adequate for the base and subbase of most types of highways in China and all types of roads in Africa. Increasing the hydrated lime dosage to 3%, 6%, and 9% further increased the CBR to 162%, 179%, and 215%, respectively. The CBR of the lime-treated soil was at least 2–3 times that of the untreated soil, meeting the standards of West Africa. When the hydrated lime and ZL-2A stabilizer were added to the granular lateritic soil, the CBR increased with the ZL-2A stabilizer content up to 0.2% but decreased for ZL-2A stabilizer contents above 0.2%.

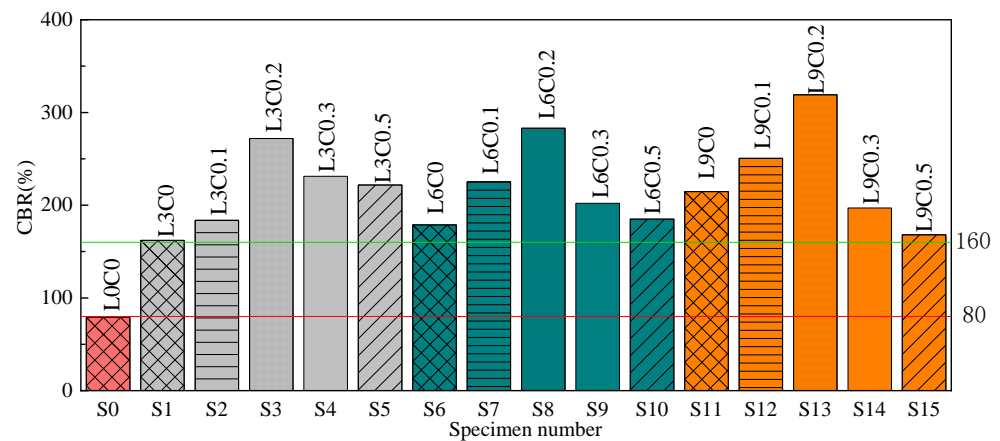


Figure 7. CBRs of the lime- and ZL-2A-stabilizer-treated granular lateritic soils.

Figure 8 shows the swelling behavior of both the raw and treated granular lateritic soils, with the measured swellings being below 0.06%. These values are far lower than the 10% swell requirement specified in the Brazilian general granular base specification. The CBR results obtained in this study are superior to those reported in numerous previous studies [14], which could be attributed to differences in the particle sizes and mineralogical composition of the raw lateritic soil [36]. Specifically, the granular lateritic soil examined in this study was relatively less rich in clay minerals.

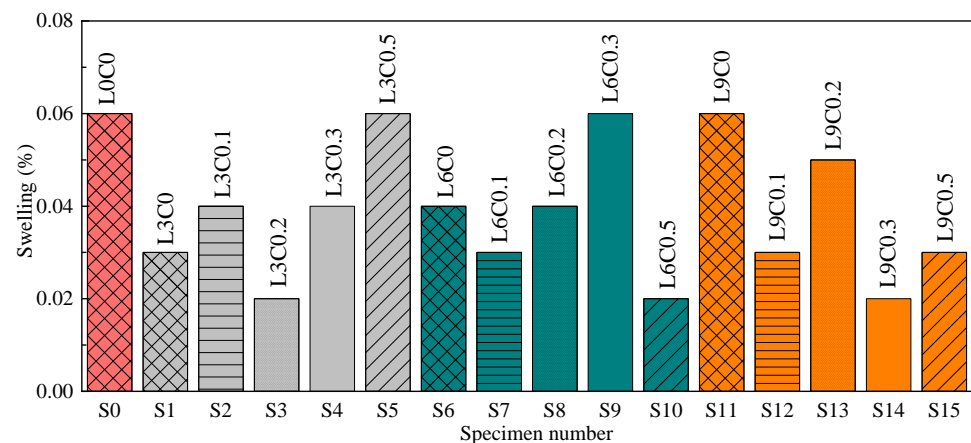


Figure 8. Swellings of lime- and ZL-2A-stabilizer-treated granular lateritic soils.

3.3. UCS

Figure 9 depicts a representative unconfined compression strength (UCS) test conducted on the treated granular lateritic soil. During the loading process, dilation deformation and vertical cracks were observed in the middle of the soil sample, as evidenced by Figure 9b. As the vertical displacement increased, the sample ultimately failed, causing the soil aggregates to drop. This phenomenon may be attributed to the predominance of calcium ion exchange reactions occurring on the surface of the granular lateritic soil particles, rather than within the lateritic clay soil [36].

Figure 10 depicts the stress–strain characteristics of the raw and treated granular lateritic soils. All of the stress–strain relationships exhibit strain-softening behavior under unconfining pressure conditions, with the stress–strain curve featuring three distinct stages: an initial slow hardening stage, a rapid linear increase stage, and a rapid drop stage. The lime-treated soils exhibit stress–strain relationships that are similar to one another, while the lime and ZL-2A-stabilized soils show differences in their stress–strain relationships, particularly with respect to their strain responses. This suggests that the addition of

the ZL-2A stabilizer improves the soil's resilience ability and makes it more resistant to deformation when compared to lime-treated lateritic soil.

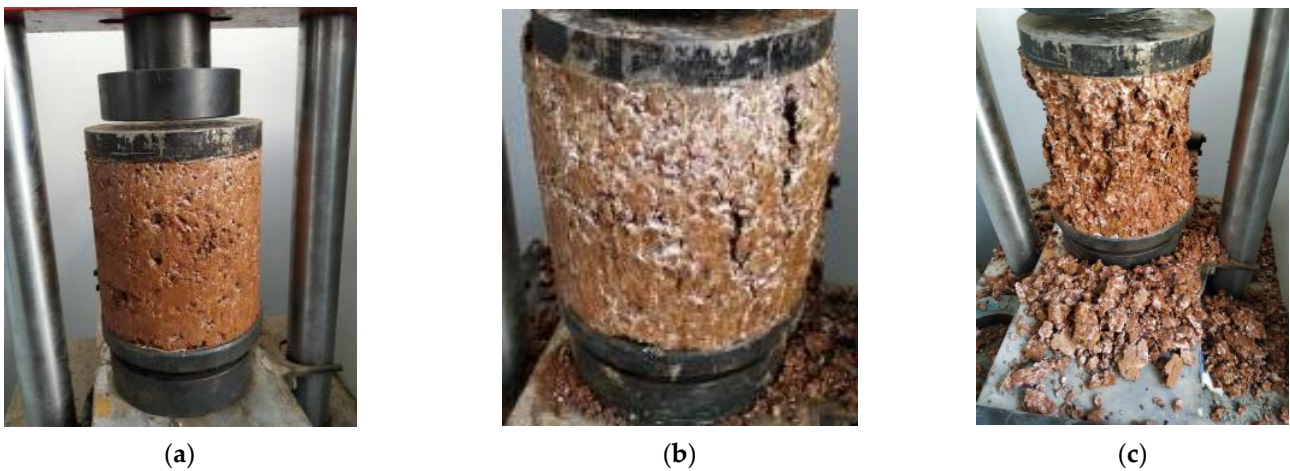


Figure 9. UCS test (S5): (a) early stage of loading; (b) mid stage of loading; (c) end of loading.

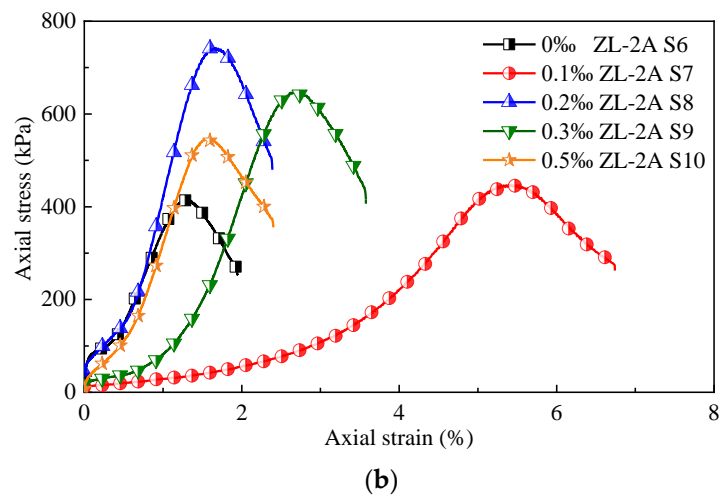
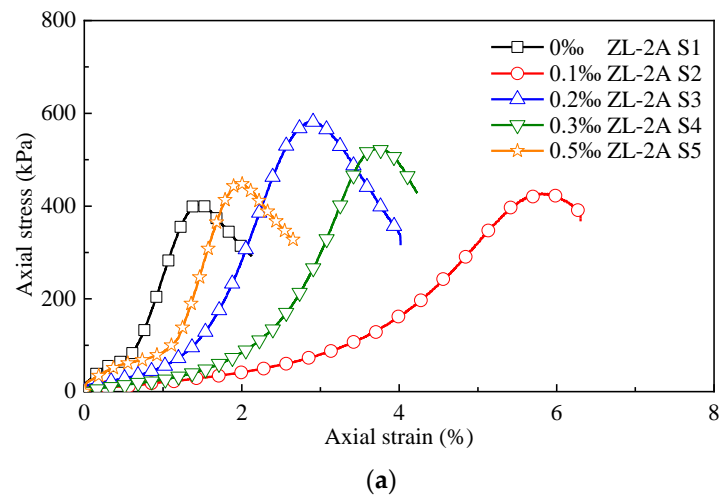


Figure 10. Cont.

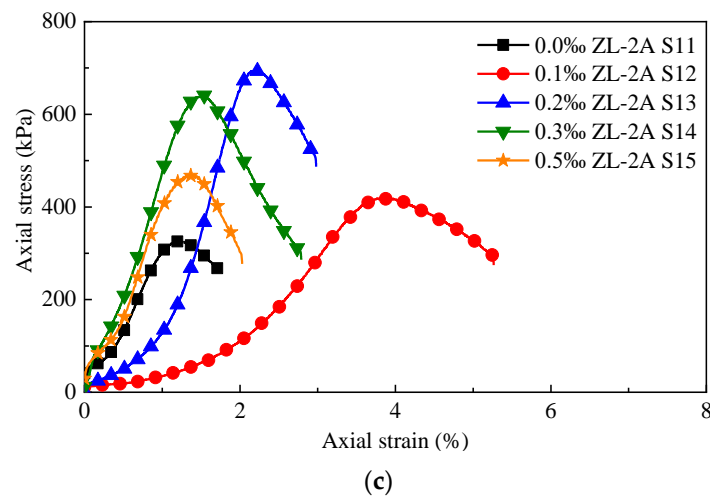


Figure 10. Stress–strain curves for the lime- and ZL-2A-stabilizer-treated granular lateritic soils: (a) 3% lime + ZL-2A stabilizer; (b) 6% lime + ZL-2A stabilizer; and (c) 9% lime + ZL-2A stabilizer.

As indicated in Figure 10a–c, when the 0.1‰ stabilizer was blended with the 3%, 6%, and 9% lime soils, the stress–strain curves displayed a slow-stage relationship, although the peak strain increased. The addition of the 0.2‰ stabilizer to the lime-treated soils caused a rapid increase in peak stress and a significant reduction in breaking strain; particularly for S8, which contained 0.2‰ stabilizer and 6% lime. For samples with stabilizer dosages of 0.3‰ and 0.5‰, the failure strains were smaller than those for samples with the 0.2‰ stabilizer.

Figure 11 presents the results of the UCS tests and the failure strains of the stabilized granular lateritic soils. The UCSs of the raw and treated soils were evaluated, and the stabilizer’s effects on the UCS were analyzed. As depicted in Figure 11a, the UCS of S1, S6, and S11 decreased from 403 to 326 kPa with an increase in lime dosage from 3% to 9%. However, the UCS increased for all samples when the ZL-2A stabilizer was added to the lime lateritic soil, with contents ranging from 0.1‰ to 0.5‰. Specifically, when the stabilizer content increased from 0.1‰ to 0.2‰, the UCS increased significantly for lime contents of 3%, 6%, and 9%. Nevertheless, the UCS decreased when the stabilizer content further increased to 0.5‰, except for S8, S13, and S3, which exhibited higher UCSs than the other samples.

Moreover, the addition of the stabilizer to the lime mixtures enhanced the failure strain by three to four times, as depicted in Figure 11b. The only-lime-treated lateritic soils exhibited smaller failure strains than those of the other samples, ranging from 1.20% to 1.44% for lime contents of 3%, 6%, and 9%. Conversely, the failure strain increased significantly to 5.8%, 5.5%, and 3.9% for the stabilizer content of 0.3‰ at lime contents of 3%, 6%, and 9%, respectively. However, the failure strain tended to decrease gradually with the increase in stabilizer content from 0.1‰ to 0.5‰, except for S4 and S9 with a stabilizer content of 0.3‰. These results indicate that the addition of the ZL-2A stabilizer significantly improved the UCS and failure strain of the stabilized granular lateritic soils, and the optimal stabilizer content could be determined based on the specific lime content used.

Figure 12 presents the test results of the 7-day UCS versus the CBR of the lime- and ZL-2A-stabilizer-treated granular lateritic soils. As shown in Figure 12, in general, CBR increases linearly with increasing 7-day UCS, which is in agreement with the linearly increasing relationship of the only-lime-treated soils or lateritic soils treated together with other binders [18,21,37]. Notably, with lower 7-day UCS, the CBR in this study is much higher than in other studies, indicating that lime- and ZL-2A-stabilizer-treated granular lateritic soils possess better stability against soaking.

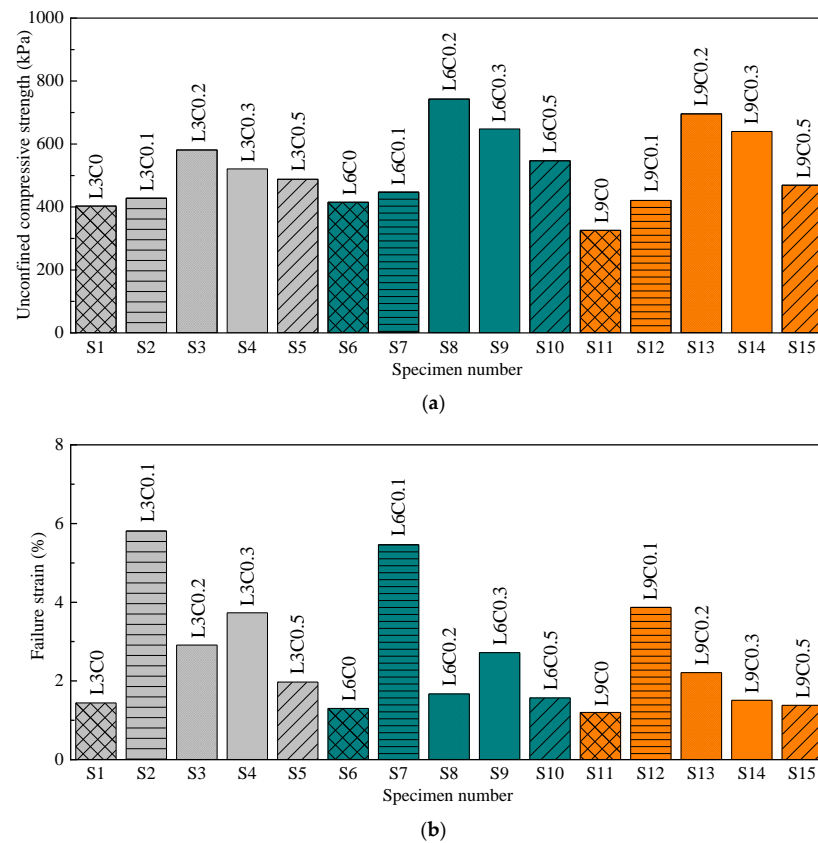


Figure 11. UCSs and failure strains of the lime- and ZL-2A-stabilizer-treated granular lateritic soils: (a) UCSs and (b) failure strain.

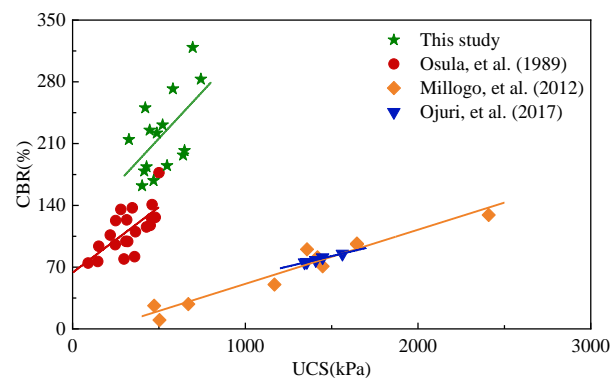


Figure 12. Relationship between the CBR and UCS [18,21,37].

4. Discussion

4.1. Mineralogical Characterization

Figure 13 shows an FTIR spectrum of the ZL-2A liquid stabilizer. The stabilizer consists of the OH hydroxyl group (3363.55 cm^{-1}), carbonyl C=O (1639.44 cm^{-1}), amino NH_2 , and hydrocarbon C–H. The main chemical component is NaOH, which can provide an alkaline reaction environment to change the surface charge distribution of the soil and facilitate the condensation reaction of clay particles in the soil. The hydroxyl groups that are hydrophilic and other functional groups that are hydrophobic form a hydrogen bond between the condensed molecules, and thus the interface state of the solution system changes significantly, and the thickness of the double electric layer is reduced, which provides an appropriate reaction environment during the curing [25,38].

Figure 14 shows the XRD patterns of the raw granular lateritic soil, hydrated lime, and treated soil with crystallite characteristics. The XRD patterns of the hydrated-lime-

treated lateritic soil show the presence of peaks at 18.4° , 34.1° , and 50.4° , which are the characteristic peaks of $\text{Ca}(\text{OH})_2$ [39]. The intensity of these peaks increased with the increasing lime content in the soil mixture. The XRD pattern of the soil treated with 6% lime and 0.2‰ stabilizer showed similar peaks to the hydrated-lime-treated soil, indicating that the stabilizer did not significantly affect the mineral composition of the soil. However, the intensity of the $\text{Ca}(\text{OH})_2$ peaks was slightly reduced compared to the hydrated-lime-treated soil, which may be due to the fact that some of the $\text{Ca}(\text{OH})_2$ was consumed during the stabilizing process [40]. The XRD patterns showed that small amounts of calcium carbonate, tricalcium silicate, tricalcium aluminate, and other cementitious minerals were formed. Overall, the XRD analysis suggests that the stabilization mechanism of the ZL-2A stabilizer is mainly physical rather than chemical.

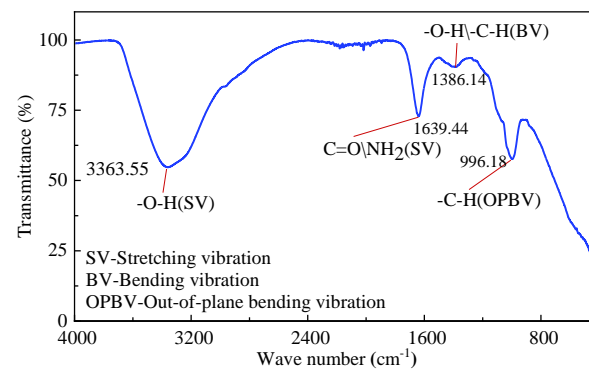


Figure 13. Infrared spectrum of the ZL-2A stabilizer.

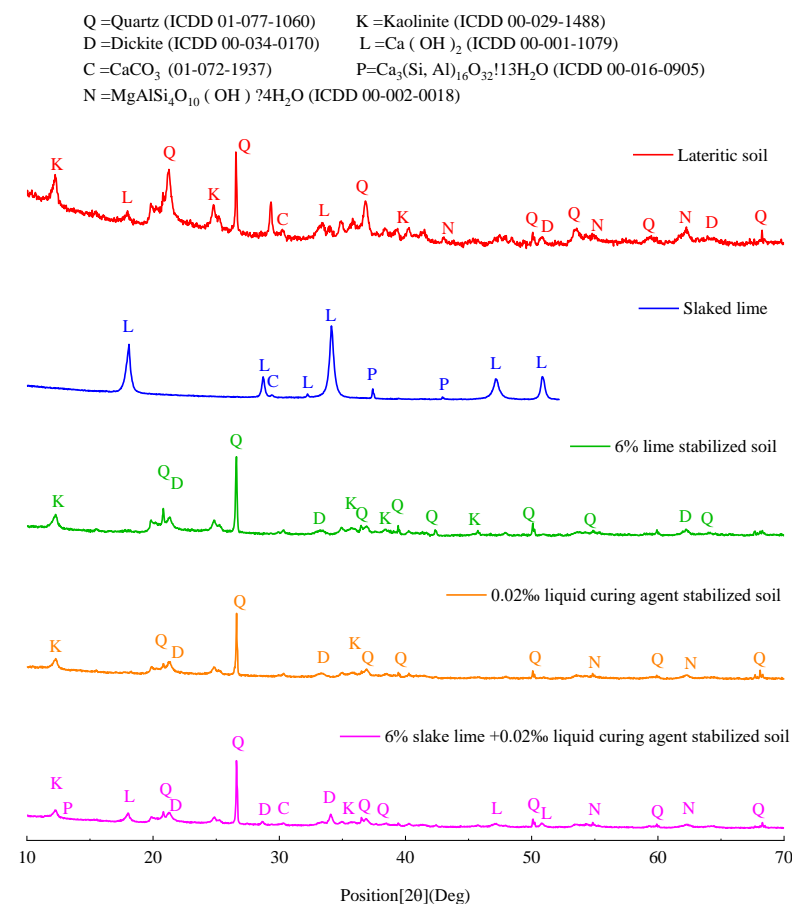


Figure 14. XRD patterns of the stabilized soils.

4.2. SEM Image Characterization

Figure 15 shows SEM images of the raw granular lateritic soil, hydrate lime, and ZL-2A stabilizer. Quartz and kaolinite were observed in the lateritic soil, which is consistent with previous research [41], and numerous calcium crystals were observed in the lime sample. The dehydrated ZL-2A stabilizer resembled a pile ball and had numerous cilia on its surface, which is a mixture of high-molecular-weight organic matter and inorganic matter such as sodium hydroxide. Macromolecular organic compounds contain hydrogen bonds that are similar to those of amides, which have a high association ability [42], high polarity, and large intermolecular forces. Therefore, it can dissolve various inorganic substances and accelerate the reaction.

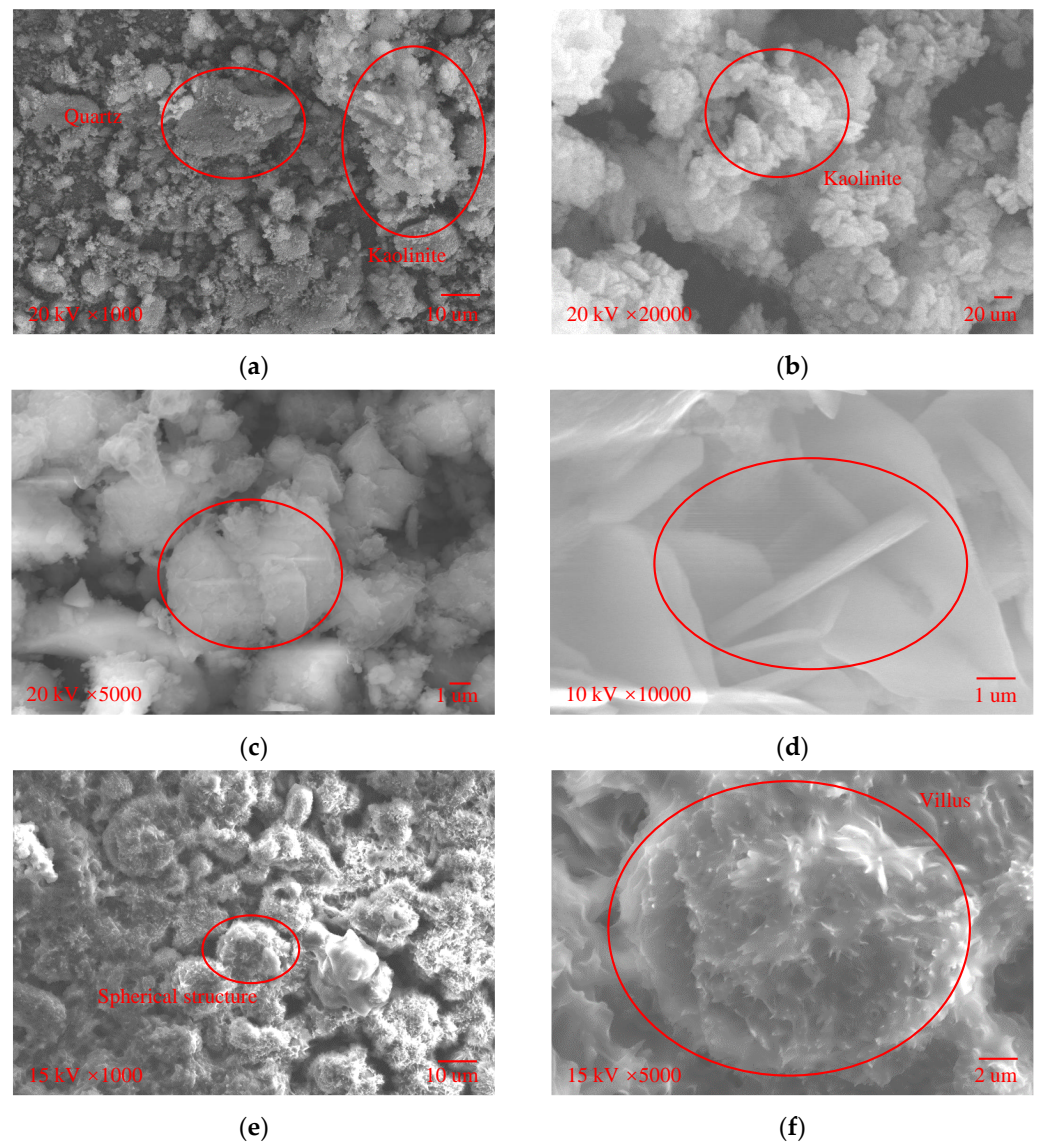


Figure 15. SEM images of the raw granular lateritic soil, hydrated lime, and ZL-2A stabilizer: (a) lateritic soils ($\times 1000$); (b) lateritic soil ($\times 20,000$); (c) hydrated lime ($\times 5000$); (d) hydrated lime ($\times 10,000$); (e) ZL-2A stabilizer ($\times 1000$); and (f) ZL-2A stabilizer ($\times 5000$).

Figure 16 shows an SEM image of the stabilized soil with the hydrated lime cured for 7 days. The large numbers of micropores and microcracks and some unreacted hydrated lime crystals adsorb clay particles. When the wet granular lateritic soil was mixed with the hydrated lime, the Ca^{2+} ions released from the calcium hydroxide were adsorbed by ion exchange at the clay mineral surface, demonstrating that the kaolinite could adsorb

calcium [43]. The diffuse hydrous double layer surrounding the clay particles can be modified by the Ca^{2+} ion exchange process, resulting in flocculation–agglomeration of clay particles among the granular lateritic particles [44]. These modifications of clay particles could enhance the interaction strength of granular lateritic particles through hydrated lime addition and improve the CBR and UCS of the soil. In addition, larger numbers of Ca^{2+} and OH^- are produced by the hydrated lime, which increases the pH of the solution and destroys silicate minerals in clay particles, destroying the micromorphology of the clay. Ca^{2+} in the hydrated lime and SiO_3^{2-} produced by silicate minerals in the clay combine to form a C-S-H product, i.e., the cluster-like particles observed in Figure 16b. Excessive hydrated lime decreases the strength of the solidified soil. Lots of hydrated lime crystals are observed in the electron microscopy image. The resulting microcracks are shown in Figure 16a.

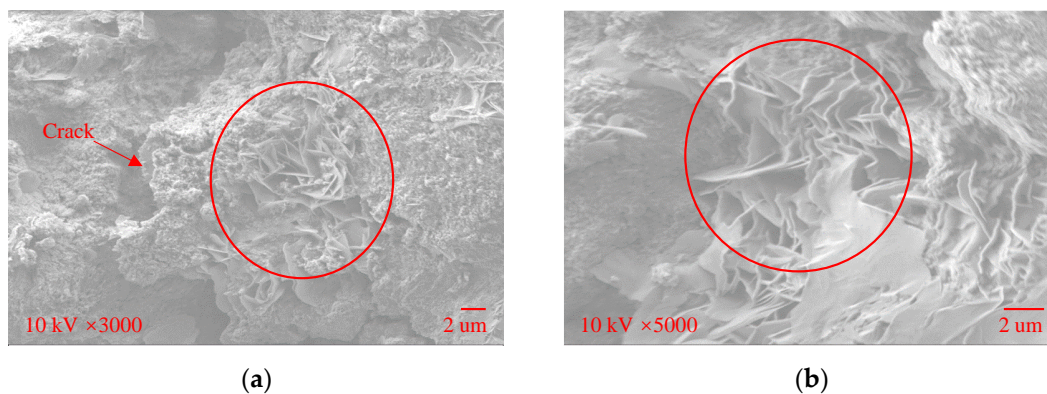


Figure 16. SEM images of the hydrated lime soil at different magnifications: (a) hydrated lime soil ($\times 3000$) and (b) hydrated lime soil ($\times 5000$).

Figure 17 shows an SEM image of the stabilized soil with the hydrated lime and ZL-2A stabilizer. The surface of the soil became rougher, and the distribution of the surface charge changed, which was beneficial for the reaction between the hydrated lime and clay particles. The gel materials in the ZL-2A stabilizer produced various underwater chemical reactions to form gelatinous hydrates, such as calcium silicate hydrate, calcium aluminate hydrate, and calcium hydroxide, which encircle soil particles (Figure 17c,d). Some of these hydrides continued to harden to form a skeleton and some reacted with soil particles to form a complex and finally connected with each other to form a stable spatial network structure (Figure 17a,b). The crystals are needle-like and are interlaced with soil aggregates (Figure 17e,f), which is similar to the effect of a connection between reinforcement and concrete, i.e., “micro-reinforcement”, which improves the strength of the solidified soil, thus enhancing the bond strength and stability between soil particles.

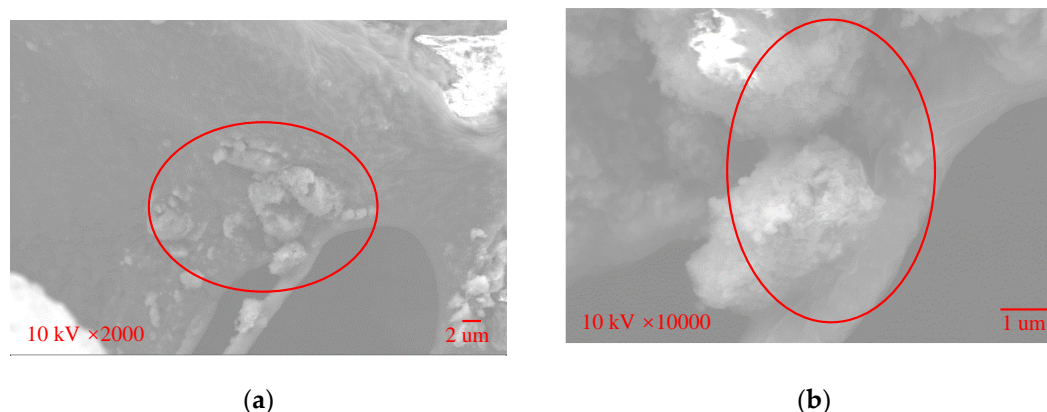


Figure 17. Cont.

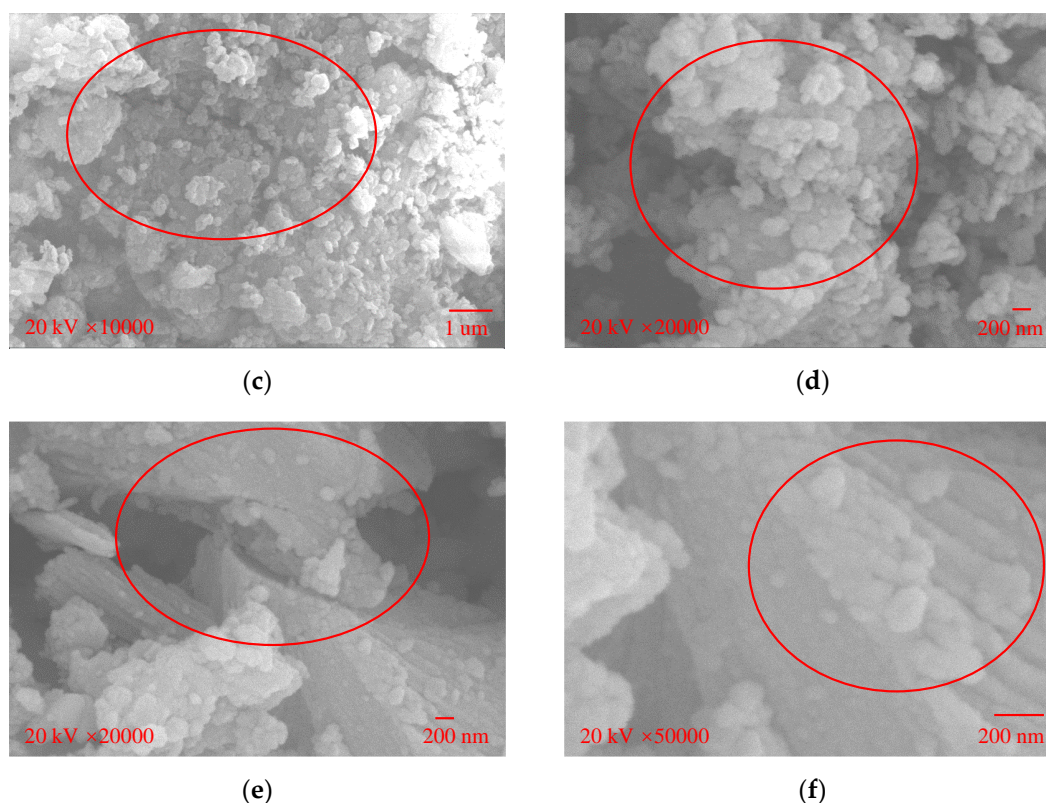


Figure 17. SEM images of hydrated lime + ZL-2A stabilizer + soil at different magnifications: (a) $\times 2000$; (b) $\times 10,000$; (c) $\times 10,000$; (d) $\times 20,000$; (e) $\times 20,000$; and (f) $\times 50,000$.

4.3. Mechanisms of Hydrated-Lime-Liquid-Stabilizer-Treated Laterite

The ion exchange between the calcium ions electrolyzed from hydrated lime and the cations in the laterite enhances the attraction between the soil particles. The calcium silicate and calcium aluminate produced by the reaction of hydrated lime with quartz, alumina, and calcium feldspar in laterite, and the hydrated calcium silicate and hydrated calcium aluminate produced by their further hydration reaction [45,46], all have strong cementing properties, which can bond the soil particles together and form a stable structure. Hence, the strength, stability, and bearing capacity of treated soil obtain a long-term improvement [47]. The liquid stabilizer can promote the hydration reaction. The sodium hydroxide contained in the liquid stabilizer could provide an alkaline environment, which could cause the change of charge distribution on the surfaces of soils, resulting in a decrease in the thickness of the electric double layer, hence benefitting the chemical reactions. Moreover, more bound water became free water with the decreasing force adsorbing water molecules induced by the ion exchange between the laterite and the liquid stabilizer, thus providing more water for the hydration reaction.

5. Conclusions

In this study, a series of indoor tests, including the compaction test, CBR test, and unconfined compressive strength test, were conducted to investigate the effects of lime and a stabilizer on laterite. In addition, the mineral composition and microstructure of stabilized laterite were analyzed using XRD and SEM tests to explore the mechanisms of stabilization. Based on the results, the following conclusions can be drawn:

- (1) The lime-stabilized laterite exhibited a CBR value of more than 160%, while the lime-liquid-stabilizer-stabilized laterite exhibited a CBR value of more than 250%, indicating that the liquid stabilizer effectively enhances the stabilization effect of lime on natural laterite. The unconfined compressive strength of the lime-liquid-

- stabilizer-stabilized laterite was at most twice that of the lime-stabilized laterite. The lime–liquid–stabilizer–stabilized laterite can be used at all layers of various subgrades.
- (2) Excessive lime and liquid stabilizer may lead to a reduction in CBR and UCS. For the laterite studied in this work, the optimum stabilization effect was achieved with a combination of 6% lime and 0.2 % liquid stabilizer. In practical engineering, it is necessary to determine the optimum dosage of lime and stabilizer.
 - (3) There is an approximately linear relationship between the CBR value and the UCS value of the stabilized laterite. Additionally, when the UCS value is far lower than that of the lime-stabilized laterite, the corresponding CBR value is almost three times that reported in the literature. These results suggest that the liquid stabilizer greatly improves the water stability of the treated laterite, demonstrating the feasibility of using a curing agent—lime—to stabilize laterite in humid Africa.
 - (4) Lime hydration results in an exchange between calcium ions and the cations in laterite, increasing the attraction between soil particles. Moreover, hydrated calcium silicate and hydrated calcium aluminate, formed by the further reaction of hydrated lime and laterite, cement soil particles together to form a stable structure. The liquid stabilizer promotes the chemical reaction between lime and soil by reducing the thickness of the double electric layer of soil particles and further improves the strength of the soil by wrapping the mixture of the granular lateritic soil and hydrated lime.

Author Contributions: The authors confirm their contribution to the paper as follows: investigation, software, and writing, K.T.; review and resources, F.Z. (Feng Zeng); supervision, L.S.; investigation, L.Z.; validation, and formal analysis, Z.C.; conception, methodology, investigation and writing, F.Z. (Feng Zhang). All authors have read and agreed to the published version of the manuscript.

Funding: This research was funded by the China Road and Bridge Corporation and National Natural Science Foundation of China, grant number 51808128.

Institutional Review Board Statement: The authors declare that this article complies with the journal's ethical standards.

Informed Consent Statement: Not applicable.

Data Availability Statement: Data is contained within the article.

Conflicts of Interest: The authors declare they have no conflicts of interest to report regarding the present study.

References

1. Gidigas, M.D. *Laterite Soil Engineering: Pedogenesis and Engineering Principles*; Elsevier: Amsterdam, The Netherlands, 2012; Volume 9.
2. Paige-Green, P.; Pinard, M.; Netterberg, F. A review of specifications for lateritic materials for low volume roads. *Trans. Geotech.* **2015**, *5*, 86–98. [[CrossRef](#)]
3. Millogo, Y.; Hajjaji, M.; Ouedraogo, R.; Gomina, M. Cement-lateritic gravels mixtures: Microstructure and strength characteristics. *Constr. Build. Mater.* **2008**, *22*, 2078–2086. [[CrossRef](#)]
4. Toll, D.G. California Bearing Ratio tests on a lateritic gravel from Kenya. *Trans. Geotech.* **2015**, *5*, 59–67. [[CrossRef](#)]
5. Magnan, J.-P.; Ndigye, M. Determination and assessment of deformation moduli of compacted lateritic gravels, using soaked CBR tests. *Trans. Geotech.* **2015**, *5*, 50–58. [[CrossRef](#)]
6. Nzabakurikiza, A.; Onana, V.L.; Ze, A.N.; Mvindi, A.T.N.; Ekodeck, G.E. Geological, geotechnical, and mechanical characterization of lateritic gravels from Eastern Cameroon for road construction purposes. *Bull. Eng. Geol. Environ.* **2017**, *76*, 1549–1562. [[CrossRef](#)]
7. Ze, A.N.; Onana, V.L.; Mvindi, A.T.N.; Ohandja, H.N.; Eko, R.M.; Ekodeck, G.E. Variability of geotechnical parameters of lateritic gravels overlying contrasted metamorphic rocks in a tropical humid area (Cameroon): Implications for road construction. *Bull. Eng. Geol. Environ.* **2019**, *78*, 5531–5549.
8. Qian, J.S.; Chen, K.W.; Tian, Y.; Zeng, F.; Wang, L. Performance evaluation of flexible pavements with a lateritic gravel base using accelerated pavement testing. *Constr. Build. Mater.* **2019**, *228*, 116790. [[CrossRef](#)]
9. Netterberg, F. *Review of Specifications for the Use of Laterite in Road Pavements*; Crown Agents: Cape Town, South Africa, 2014.
10. Biswal, D.R.; Sahoo, U.C.; Dash, S.R. Characterization of granular lateritic soils as pavement material. *Trans. Geotech.* **2016**, *6*, 108–122. [[CrossRef](#)]

11. Lim, S.M.; Yao, K.; Jiang, Y.; Lim, Z.C.; Bakar, I.H. Geotechnical characteristics of lateritic clay admixed with biomass silica stabilizer. *J. Clean. Prod.* **2021**, *321*, 129008. [[CrossRef](#)]
12. Okeke, C.; Abbey, S.; Oti, J.; Eyo, E.; Johnson, A.; Ngambi, S.; Abam, T.; Ujile, M. Appropriate use of lime in the study of the physicochemical behaviour of stabilised lateritic soil under continuous water ingress. *Sustainability* **2020**, *13*, 257. [[CrossRef](#)]
13. Saeed, K.A.; Kassim, K.A.; Nur, H.; Yunus, N.Z.M. Strength of lime-cement stabilized tropical lateritic clay contaminated by heavy metals. *KSCE J. Civ. Eng.* **2015**, *19*, 887–892. [[CrossRef](#)]
14. Billong, N.; Melo, U.C.; Louvet, F.; Njopwouo, D. Properties of compressed lateritic soil stabilized with a burnt clay–lime binder: Effect of mixture components. *Constr. Build. Mater.* **2009**, *23*, 2457–2460. [[CrossRef](#)]
15. Obianyo, I.I.; Onwualu, A.P.; Soboyejo, A.B. Mechanical behaviour of lateritic soil stabilized with bone ash and hydrated lime for sustainable building applications. *Case Stud. Constr. Mater.* **2020**, *12*, e00331. [[CrossRef](#)]
16. Osula, D. Lime modification of problem laterite. *Eng. Geol.* **1991**, *30*, 141–154. [[CrossRef](#)]
17. Osinubi, K.J. Permeability of lime-treated lateritic soil. *J. Transp. Eng.* **1998**, *124*, 465–469. [[CrossRef](#)]
18. Millogo, Y.; Morel, J.C.; Traoré, K.; Ouedraogo, R. Microstructure, geotechnical and mechanical characteristics of quicklime-lateritic gravels mixtures used in road construction. *Constr. Build. Mater.* **2012**, *26*, 663–669. [[CrossRef](#)]
19. Eisazadeh, A.; Kassim, K.A.; Nur, H. Solid-state NMR and FTIR studies of lime stabilized montmorillonitic and lateritic clays. *Appl. Clay Sci.* **2012**, *67–68*, 5–10. [[CrossRef](#)]
20. Tan, Y.; Hu, M.; Li, D. Effects of agglomerate size on california bearing ratio of lime treated lateritic soils. *Int. J. Sustain. Built Environ.* **2016**, *5*, 168–175. [[CrossRef](#)]
21. Ojuri, O.O.; Adavi, A.A.; Oluwatuyi, O.E. Geotechnical and environmental evaluation of lime-cement stabilized soil-mine tailing mixtures for highway construction. *Trans. Geotech.* **2017**, *10*, 1–12. [[CrossRef](#)]
22. Amulya, G.; Moghal, A.A.B.; Almajed, A. Sustainable Binary Blending for Low-Volume Roads—Reliability-Based Design Approach and Carbon Footprint Analysis. *Materials* **2023**, *16*, 2065. [[CrossRef](#)]
23. Katz, L.E.; Rauch, A.F.; Liljestrang, H.M.; Harmon, J.S.; Shaw, K.S.; Albers, H. Mechanisms of soil stabilization with liquid ionic stabilizer. *Transp. Res. Rec.* **2001**, *1757*, 50–57. [[CrossRef](#)]
24. Liu, J.; Shi, B.; Jiang, H.; Huang, H.; Wang, G.; Kamai, T. Research on the stabilization treatment of clay slope topsoil by organic polymer soil stabilizer. *Eng. Geol.* **2011**, *117*, 114–120. [[CrossRef](#)]
25. Xiang, W.; Cui, D.; Liu, Q.; Lu, X.; Cao, L. Theory and practice of ionic soil stabilizer reinforcing special clay. *J. Earth Sci.-China* **2010**, *21*, 882–887. [[CrossRef](#)]
26. He, S. *Chemical Stabilization of Expansive Soils Using Liquid Ionic Soil Stabilizers (LISS)*; The University of Texas at Arlington: Austin, TX, USA, 2019.
27. Sarkar, S.L.; Herbert, B.E.; Scharlin, R.J. Injection stabilization of expansive clays using a hydrogen ion exchange chemical. In *Advances in Unsaturated Geotechnics*; American Society of Civil Engineers: Reston, VA, USA, 2000; pp. 487–516.
28. Yunus, N.Z.M.; Yung, Y.C.; Wei, N.T.; Abdullah, N.; Mashros, N.; Kadir, M.A.A. Shear strength behaviour of canlite-treated laterite soil. *J. Teknol.* **2015**, *72*, 91–97.
29. Gullu, H.; Hazirbaba, K. Unconfined compressive strength and post-freeze–thaw behavior of fine-grained soils treated with geofiber and synthetic fluid. *Cold Reg. Sci. Technol.* **2010**, *62*, 142–150. [[CrossRef](#)]
30. Zhao, H.; Ge, L.; Petry, T.M.; Sun, Y.Z. Effects of chemical stabilizers on an expansive clay. *KSCE J. Civ. Eng.* **2014**, *18*, 1009–1017. [[CrossRef](#)]
31. Gautam, S.; Hoyos, L.R.; He, S.; Prabakar, S.; Yu, X. Chemical treatment of a highly expansive clay using a liquid ionic soil stabilizer. *Geotech. Geol. Eng.* **2020**, *38*, 4981–4993. [[CrossRef](#)]
32. Wu, X.T.; Sun, J.S.; Qi, Y.; Chen, B. Pore and compression characteristics of clay solidified by ionic soil stabilizer. *Bull. Eng. Geol. Environ.* **2021**, *80*, 5003–5019. [[CrossRef](#)]
33. *JTG 3430-2020; Test Methods of Soils for Highway Engineering*. Ministry of Transport of the People’s Republic of China: Beijing, China, 2020.
34. *GB 7817-1987; Total Analysis Methods of Forest Soil (GB 7873-87)*. National Bureau of Standards: Beijing, China, 1987.
35. *JTG E51-2009; Test Methods of Materials Stabilised with Inorganic Binders for Highway Engineering*. Ministry of Transport of the People’s Republic of China: Beijing, China, 2009.
36. Wang, Y.; Duc, M.; Cui, Y.J.; Tang, A.M.; Benahmed, N.; Sun, W.J.; Ye, W.M. Aggregate size effect on the development of cementitious compounds in a lime-treated soil during curing. *Appl. Clay Sci.* **2017**, *136*, 58–66. [[CrossRef](#)]
37. Osula, D.O. Evaluation of admixture stabilization for problem laterite. *J. Transp. Eng.* **1989**, *115*, 674–687. [[CrossRef](#)]
38. Tingle, J.S.; Newman, J.K.; Larson, S.L.; Weiss, C.A.; Rushing, J.F. Stabilization mechanisms of nontraditional additives. *Transp. Res. Rec.* **2007**, *1989*, 59–67. [[CrossRef](#)]
39. Vu, H.H.T.; Gu, S.; Thriveni, T.; Khan, M.D.; Tuan, L.Q.; Ahn, J.W. Sustainable treatment for sulfate and lead removal from battery wastewater. *Sustainability* **2019**, *11*, 3497. [[CrossRef](#)]
40. Al-Mukhtar, M.; Lasledj, A.; Alcover, J.F. Lime consumption of different clayey soils. *App. Clay Sci.* **2014**, *95*, 133–145. [[CrossRef](#)]
41. Vilhena, R.M.; Mascarenha, M.M.D.A.; Angelim, R.R.; Simões, T.D.R.; Oliveira, R.B.D.; Luz, M.P.D. Evaluation of lime-treated lateritic soil for reservoir shoreline stabilization. *Water* **2020**, *12*, 3141. [[CrossRef](#)]
42. Johansson, A.; Kollman, P.; Rothenberg, S.; McKelvey, J. Hydrogen bonding ability of the amide group. *J. Am. Chem. Soc.* **1974**, *96*, 3794–3800. [[CrossRef](#)]

43. Chemedda, Y.C.; Deneele, D.; Ouvrard, G. Short-term lime solution-kaolinite interfacial chemistry and its effect on long-term pozzolanic activity. *Appl. Clay Sci.* **2018**, *161*, 419–426. [[CrossRef](#)]
44. Chavali, R.V.P.; Vindula, S.K.; Babu, A.; Pillai, R.J. Swelling behavior of kaolinitic clays contaminated with alkali solutions: A micro-level study. *Appl. Clay Sci.* **2017**, *135*, 575–582. [[CrossRef](#)]
45. Al-Mukhtar, M.; Lasledj, A.; Alcover, J.F. Behaviour and mineralogy changes in lime-treated expansive soil at 20 C. *Appl. Clay Sci.* **2010**, *50*, 191–198. [[CrossRef](#)]
46. Federico, A.; Vitone, C.; Murianni, A. On the mechanical behaviour of dredged submarine clayey sediments stabilized with lime or cement. *Can. Geotech. J.* **2015**, *52*, 2030–2040. [[CrossRef](#)]
47. Rosone, M.; Celauro, C.; Ferrari, A. Microstructure and shear strength evolution of a lime-treated clay for use in road construction. *Int. J. Pavement Eng.* **2020**, *21*, 1147–1158. [[CrossRef](#)]

Disclaimer/Publisher's Note: The statements, opinions and data contained in all publications are solely those of the individual author(s) and contributor(s) and not of MDPI and/or the editor(s). MDPI and/or the editor(s) disclaim responsibility for any injury to people or property resulting from any ideas, methods, instructions or products referred to in the content.